EPJ Web of Conferences **339**, 04006 (2025) https://doi.org/10.1051/epjconf/202533904006
Hard Probes 2024

Measurements of charmonium production in heavy-ion collisions at STAR

Wei Zhang[1,*], for the STAR Collaboration

[1]South China Normal University

Abstract. In this proceeding, we presented the nuclear modification factor (R_{AA}) of J/ψ as a function of centrality and transverse momentum in Au+Au collisions at $\sqrt{s_{\rm NN}}$ = 14.6, 17.3, 19.6, and 27 GeV collected by STAR. The energy dependence of J/ψ R_{AA} from RHIC to LHC energies is also investigated, and compared with model calculations. Additionally, the first measurement of ψ(2S) production in isobaric collisions at top RHIC energy is presented, including the centrality and transverse momentum dependence of the ψ(2S) over J/ψ yield ratio.

1 Introduction

In relativistic heavy-ion collisions, the dissociation of charmonium is regarded as a key signature of quark-gluon plasma (QGP) formation [1, 2]. The suppression of charmonium production in such environments is attributed to the deconfinement of quarks and gluons, which leads to the breakup of bound states like J/ψ. However, in addition to dissociation, charmonium also experiences a regeneration effect within the QGP [3]. Regeneration refers to the process in which uncorrelated quarks and antiquarks combine to form a bound state in the medium, which partially compensates for the suppression. Additionally, cold nuclear matter (CNM) effects, such as nuclear absorption and parton shadowing, further influence charmonium production. The interplay of dissociation, regeneration, and CNM effects complicates the interpretation of experimental results.

As the collision energy decreases, the regeneration effect weakens rapidly, allowing a cleaner study of contributions from dissociation and CNM effects. This provides a good opportunity to study the QGP properties, particularly at lower energies. Additionally, different quarkonium states, such as J/ψ and $\psi(2S)$, are expected to dissociate at different temperatures due to their varying binding energies. The suppression of these states follows an ordered pattern, where states with weaker binding energies, such as $\psi(2S)$, are more likely to dissociate, while more tightly bound states, such as J/ψ, exhibit greater resistance to suppression. This sequential suppression offers insights into the medium's screening effects and deconfinement properties.

2 Dataset

The data analyzed in this study were collected by the RHIC-STAR experiment at Brookhaven National Laboratory. As part of the Beam Energy Scan-II (BES-II) program—Au+Au (gold-gold) collisions at $\sqrt{s_{\rm NN}}$ = 14.6, 17.3, 19.6, and 27 GeV were recorded during the 2019,

*e-mail: wzhang@m.scnu.edu.cn

2021, and 2018 RHIC runs. These data were analyzed to investigate J/ψ suppression. Additionally, the STAR detector collected Ru+Ru and Zr+Zr (isobar) collision data during the 2018 RHIC run at $\sqrt{s_{\rm NN}}$ = 200 GeV, which are utilized to study the sequential suppression of charmonium.

3 Analysis detail

3.1 Nuclear modification factor

The J/ψ candidates are reconstructed via the di-electron channel. Event and track quality selections are applied. Electrons are identified using a combination of the specific energy loss (dE/dx) measured by the Time Projection Chamber (TPC) and the particle velocity (β) from the Time-of-Flight (TOF) detector. Slow hadrons are rejected with TOF, and an additional dE/dx cut is applied to further suppress residual hadronic contamination, particularly from pions.The raw J/ψ yields are extracted by fitting the invariant mass distribution of electron pairs with the J/ψ shape obtained from a toy Monte Carlo (MC) simulation that incorporates detector effects. This ensures that the template accurately reflects the detector resolution and acceptance. The fit determines the normalization of the signal template, which corresponds to the raw J/ψ yield. The yields are then corrected for detector acceptance and efficiency, evaluated using a combination of embedding and data-driven methods.

The nuclear modification factor (R_{AA}) is used to quantify the suppression of J/ψ production and is defined as:

$$R_{AA} = \frac{d^2N^{AA}/dp_{\rm T}dy}{\langle T_{AA}\rangle \times d^2\sigma^{pp}/dp_{\rm T}dy} \tag{1}$$

Here, $d^2N_{AA}/dp_{\rm T}dy$ represents the J/ψ yield in A+A collisions, while $d^2\sigma_{pp}/dp_{\rm T}dy$ denotes the J/ψ cross section in $p+p$ collisions. Since no experimental data are available, the J/ψ production cross section in $p+p$ collisions at $\sqrt{s_{\rm NN}}$ = 14.6, 17.3, 19.6, and 27 GeV is derived using a data-driven approach based on global experimental data from $p+p$ to $p+A$ collisions [4]. The nuclear overlap function T_{AA}, which characterizes the collision geometry and density, is calculated via the Glauber model.

3.2 $\psi(2S)$ to J/ψ ratio

The $\psi(2S)$ and J/ψ production in isobar collisions were also reconstructed through the di-electron channel. However, despite the high-statistics isobar collision data collected by the STAR experiment, extracting the $\psi(2S)$ signal remained challenging due to its small cross section at RHIC energies and significant background contamination. To address this, a machine learning approach was applied to enhance the signal-to-background ratio. The $\psi(2S)$ signal is clearly resolved in the invariant mass distribution shown in Fig. 1, reconstructed through the dielectron decay channel within $|y| < 1$ and $p_{\rm T} > 0.2$ GeV/c. The solid black curves represent fits to the filled black circles, which correspond to the dielectron signal after subtraction of the combinatorial background using the mixed-event technique. Curves with different line styles represent individual fit components, while the pink curve denotes the residual background from sources such as heavy-flavor decays and Drell–Yan processes in the $\psi(2S)$ mass region. The width of the pink band indicates the uncertainty arising from the fit.

Once the $\psi(2S)$ signal was obtained, the $\psi(2S)$ to J/ψ yield ratio was determined as a function of $N_{\rm part}$ and $p_{\rm T}$, which can then be compared between A+A and $p+p$ collisions.

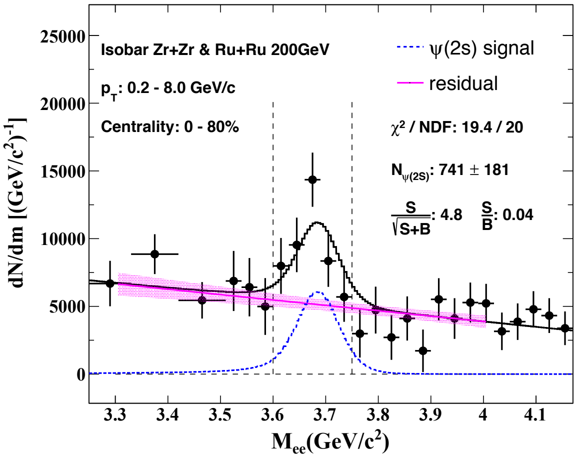

Figure 1. Invariant mass distributions of $\psi(2S)$ candidates for $p_T > 0.2$ GeV/c, reconstructed via the dielectron channel within $|y| < 1$ for 0–80% Ru+Ru and Zr+Zr collisions. The background-subtracted distributions (black circles) are fitted. The fit results are shown by the solid black curves, while the pink curves represent the residual background components and the blue dashed line represents the $\psi(2S)$ signal component. The mass ranges used to determine the signal counts are indicated by the shaded bands.

4 Results

4.1 BES-II J/ψ R_{AA} result

The inclusive J/ψ R_{AA} as a function of the number of participants ($N_{\rm part}$) in Au+Au collisions at $\sqrt{s_{\rm NN}}$ = 14.6, 17.3, 19.6, and 27 GeV at mid-rapidity ($|y| < 1$), compared to 200 GeV [5], is presented in the left panel of Fig. 2. A stronger suppression is observed with increasing $N_{\rm part}$, which follows a similar trend to the 200 GeV results.

The right panel of Fig. 2 shows the inclusive J/ψ R_{AA} as a function of transverse momentum ($p_{\rm T}$) for centrality-integrated results, compared to 200 GeV. For the data below 200 GeV, a clear $p_{\rm T}$ dependence is observed: suppression is strongest at low $p_{\rm T}$, and R_{AA} rises with increasing $p_{\rm T}$. This low-$p_{\rm T}$ suppression may partially arise from CNM effects, which are expected to contribute more significantly at the lower collision energies studied here than at 200 GeV. Although low-$p_{\rm T}$ suppression also appears at 200 GeV, the trend there is much flatter, suggesting that a not-negligible regeneration contribution at 200 GeV more effectively offsets suppression at low $p_{\rm T}$.

Fig. 3 presents the R_{AA} as a function of collision energy in central collisions [5–10]. Notably, no clear energy dependence is observed for collision energy below 200 GeV, suggesting that the competing mechanisms (such as dissociation, regeneration, and CNM effects) counterbalance each other within this energy range. At lower energies, CNM effects are expected to play a more significant role, while at higher energies, regeneration becomes increasingly important owing to enhanced charm quark density. Furthermore, model calculations [11] incorporating these effects qualitatively reproduce the overall trend of the data but tend to underestimate the suppression at $\sqrt{s_{\rm NN}} < 27$ GeV, indicating potential missing contributions or limitations in the theoretical framework.

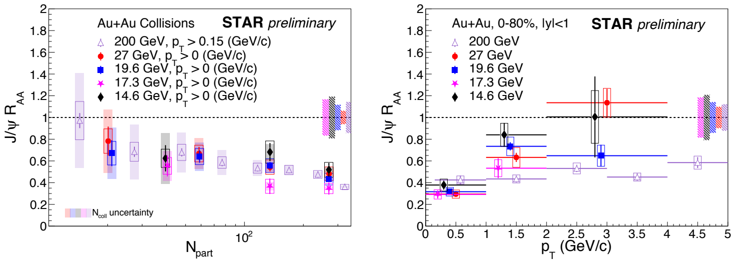

Figure 2. The inclusive J/ψ R_{AA} as a function of N_{part} (left) and p_{T} (right) at mid-rapidity for Au+Au collisions at $\sqrt{s_{\mathrm{NN}}}$ = 14.6, 17.3, 19.6, and 27 GeV is compared to results at 200 GeV. In both panels, vertical bars and open boxes around data points represent statistical and systematic uncertainties, respectively. Filled boxes around unity indicate global uncertainties from the $p+p$ baselines (left panel) and the $p+p$ baseline combined with T_{AA} (right panel). Shaded bands on data points (left) reflect uncertainties from T_{AA}. For clarity, the p_{T} positions of the 14.6, 17.3, and 19.6 GeV data in the right panel are slightly shifted.

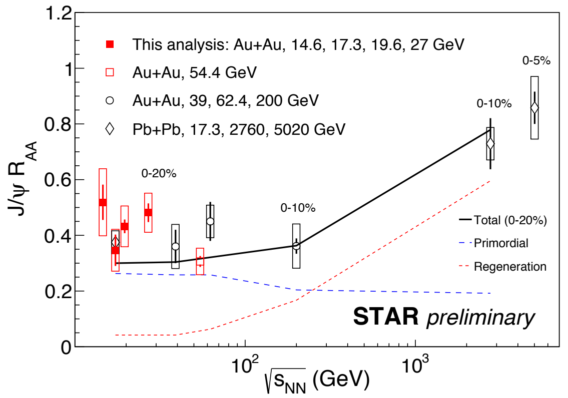

Figure 3. The R_{AA} of J/ψ as a function of collision energy for central collisions is compared with model calculations. The vertical bars represent statistical uncertainties, while the open boxes around data points represent systematic uncertainties, including those from heavy-ion measurements, $p+p$ baselines and N_{coll}.

4.2 Charmonium sequential suppression

The $\psi(2S)$ to J/ψ double ratio, as defined in Equation 2, is shown in the left panel of Fig. 4. The red solid points represent the newly measured results, marking the first observation of charmonium sequential suppression in heavy-ion collisions at RHIC. These results exhibit a hint of decreasing trend as a function of N_{part}, and are consistent with both the SPS results [12] (Pb+Pb at $\sqrt{s_{\mathrm{NN}}} = 17.3$ GeV, $0 < y < 1$) and the LHC results [3] (Pb+Pb at $\sqrt{s_{\mathrm{NN}}} = 5.02$ TeV, $2.5 < y < 4$). The double ratio is significantly lower than 1 in central collisions, indicating a stronger suppression of the $\psi(2S)$ relative to the J/ψ in heavy-ion (A+A) collisions compared to proton-proton ($p+p$) collisions.

The right panel of Fig. 4 shows the $\psi(2S)$ to J/ψ yield ratio as a function of p_{T} in isobar collisions at $\sqrt{s_{\mathrm{NN}}}$ = 200 GeV, compared with world-wide $p+p$ and $p+A$ results. In all cases (isobar, $p+p$, and $p+A$ collisions), the $\psi(2S)$ to J/ψ yield exhibits a hint of increasing trend with p_T. However, for $p_T < 2$ GeV/c, the ratio is significantly lower in isobar collisions than that in $p+p$ and $p+A$ collisions, suggesting that the medium generated in isobar collisions plays a key role in the suppression of the $\psi(2S)$ state.

$$\frac{\left(\frac{Bd\sigma_{\psi(2S)}}{Bd\sigma_{J/\psi}}\right)_{AA}}{\left(\frac{Bd\sigma_{\psi(2S)}}{Bd\sigma_{J/\psi}}\right)_{pp,pd}} \tag{2}$$

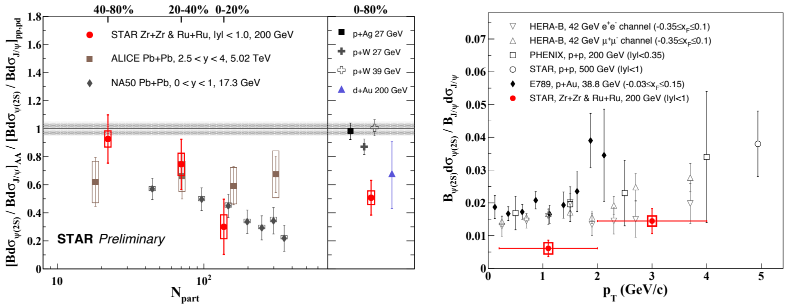

Figure 4. Left panel: The inclusive $\psi(2S)$ to J/ψ double ratio as a function of $\langle N_{\text{part}}\rangle$ is compared to previous results. For heavy-ion collision measurements [3, 12], statistical uncertainties are represented by error bars, while systematic uncertainties are shown as boxes. Other results provide only total errors [13–15]. The reference baseline for $p+p$ is derived from a combination of results in [16–18]. Right panel: The dependence of the $\psi(2S)$ to J/ψ yield ratio on p_T in $p+p$[16, 19], $p+A$[20, 21], and $A+A$ (this result) collisions. The bars and boxes indicate statistical and systematic uncertainties, respectively.

5 Summary

In this contribution, we report the measurements of the nuclear modification factor (R_{AA}) for J/ψ production in Au+Au collisions at $\sqrt{s_{\text{NN}}}$ = 14.6, 17.3, 19.6, and 27 GeV at STAR. We observe no significant energy dependence of R_{AA} for $\sqrt{s_{\text{NN}}}$ below 200 GeV. Additionally, we present the first measurement of $\psi(2S)$ production in isobar collisions at $\sqrt{s_{\text{NN}}}$ = 200 GeV, providing the first evidence of charmonium sequential suppression at RHIC. The $\psi(2S)$ to J/ψ yield ratio is significantly lower in isobar collisions compared to that in proton-proton and proton-nucleus collisions. Furthermore, the $\psi(2S)$ to J/ψ yield ratio shows a hint of increasing trend with p_T in isobar collisions, with suppression observed at low p_T values. These results provide new insights into the suppression mechanisms of charmonium states in heavy-ion collisions and contribute to a deeper understanding of the quark-gluon plasma.

References

[1] A. Andronic, R. Arnaldi, Quarkonia and Deconfined Quark-Gluon Matter in Heavy-Ion Collisions (2025), `2501.08290`.

[2] T. Matsui, H. Satz, J/ψ Suppression by Quark-Gluon Plasma Formation, Phys. Lett. B **178**, 416 (1986). 10.1016/0370-2693(86)91404-8

[3] H. Hushnud (ALICE), Measurements of ψ(2S) production in Pb–Pb collisions with ALICE at the LHC, PoS **LHCP2022**, 267 (2023). 10.22323/1.422.0267

[4] W. Zha, B. Huang, R. Ma, L. Ruan, Z. Tang, Z. Xu, C. Yang, Q. Yang, S. Yang, Systematic study of the experimental measurements on J/ψ cross sections and kinematic distributions in p+p collisions at different energies, Phys. Rev. C **93**, 024919 (2016), 1506.08985. 10.1103/PhysRevC.93.024919

[5] J. Adam et al. (STAR), Measurement of inclusive J/ψ suppression in Au+Au collisions at $\sqrt{s_{NN}}$ = 200 GeV through the dimuon channel at STAR, Phys. Lett. B **797**, 134917 (2019), 1905.13669. 10.1016/j.physletb.2019.134917

[6] M.C. Abreu et al. (NA50), Evidence for deconfinement of quarks and gluons from the J / psi suppression pattern measured in Pb + Pb collisions at the CERN SPS, Phys. Lett. B **477**, 28 (2000). 10.1016/S0370-2693(00)00237-9

[7] L. Kluberg, 20 years of J/psi suppression at the CERN SPS: Results from experiments NA38, NA51 and NA50, Eur. Phys. J. C **43**, 145 (2005). 10.1140/epjc/s2005-02245-6

[8] B.B. Abelev et al. (ALICE), Centrality, rapidity and transverse momentum dependence of J/ψ suppression in Pb-Pb collisions at $\sqrt{s_{\rm NN}}$=2.76 TeV, Phys. Lett. B **734**, 314 (2014), 1311.0214. 10.1016/j.physletb.2014.05.064

[9] L. Adamczyk et al. (STAR), Energy dependence of J/ψ production in Au+Au collisions at $\sqrt{s_{NN}}$ = 39, 62.4 and 200 GeV, Phys. Lett. B **771**, 13 (2017), 1607.07517. 10.1016/j.physletb.2017.04.078

[10] X. Bai (ALICE), Quarkonium measurements in nucleus-nucleus collisions with ALICE, Nucl. Phys. A **1005**, 121769 (2021), 2001.11925. 10.1016/j.nuclphysa.2020.121769

[11] X. Zhao, R. Rapp, Charmonium in medium: from correlators to experiment, Physical Review C—Nuclear Physics **82**, 064905 (2010).

[12] B. Alessandro et al. (NA50), psi-prime production in Pb-Pb collisions at 158-GeV/nucleon, Eur. Phys. J. C **49**, 559 (2007), nucl-ex/0612013. 10.1140/epjc/s10052-006-0153-y

[13] B. Alessandro et al. (NA50), J/psi and psi-prime production and their normal nuclear absorption in proton-nucleus collisions at 400-GeV, Eur. Phys. J. C **48**, 329 (2006), nucl-ex/0612012. 10.1140/epjc/s10052-006-0079-4

[14] A. Adare et al. (PHENIX), Nuclear Modification of ,$_c$, and J/ψ Production in d+Au Collisions at $\sqrt{s_{NN}}$=200 GeV, Phys. Rev. Lett. **111**, 202301 (2013), 1305.5516. 10.1103/PhysRevLett.111.202301

[15] D.M. Alde et al., The A-Dependence of J/ψ and ψ' Production at 800 GeV/c, Phys. Rev. Lett. **66**, 133 (1991). 10.1103/PhysRevLett.66.133

[16] P. collaboration et al., A. adare et al., ground and excited charmonium state production in p+ p collisions at s= 200 gev, Phys. Rev. D **85**, 092004 (2012).

[17] M.C. Abreu et al. (NA51), J / psi, psi' and Drell-Yan production in p p and p d interactions at 450-GeV/c, Phys. Lett. B **438**, 35 (1998). 10.1016/S0370-2693(98)01014-4

[18] A.G. Clark et al., Electron Pair Production at the CERN ISR, Nucl. Phys. B **142**, 29 (1978). 10.1016/0550-3213(78)90400-5

[19] B. Trzeciak (STAR), J/ψ and $\psi(2S)$ measurement in p+p collisions at $\sqrt{s}$ = 200 and 500 GeV in the STAR experiment, J. Phys. Conf. Ser. **612**, 012038 (2015), 1412.7341. 10.1088/1742-6596/612/1/012038

[20] I. Abt et al. (HERA-B), A Measurement of the ψ' to J/ψ production ratio in 920-GeV proton-nucleus interactions, Eur. Phys. J. C **49**, 545 (2007), hep-ex/0607046. 10.1140/epjc/s10052-006-0139-9

[21] M.H. Schub et al. (E789), Measurement of J/ψ and ψ' production in 800-GeV/c proton - gold collisions, Phys. Rev. D **52**, 1307 (1995), [Erratum: Phys.Rev.D 53, 570 (1996)]. 10.1103/PhysRevD.53.570